

The mutual interaction of powerful radio galaxies and their environments

Christian R. Kaiser¹

Astrophysics Department, Oxford University, Keble Road, Oxford, OX1 3RH, UK.

Paul Alexander

MRAO, Cavendish Lab., Madingley Road, Cambridge, CB3 0HE, UK.

Abstract. Using a self-similar model for the expansion of cocoons surrounding the jets in powerful extragalactic radio sources (type FR II), we investigate the influence of the properties of the gas surrounding these objects on their evolution. The variation of their radio luminosity as a function of linear size for individual sources is determined in dependence of the density distribution of the IGM the source is embedded in. Based on these results, the cosmological evolution of the FR II population and hence that of the environments of these sources can be constrained. The environments are found to be denser and/or more extended at high redshifts. The bow shock surrounding the cocoon of FR II sources compresses and heats the IGM. A numerical integration of the hydrodynamic equations governing the gas flow between the bow shock and the cocoon boundary is presented. From this we determine the appearance of the large scale structure of radio galaxies in X-rays and the cooling times for the IGM heated by the passage of the bow shock. This has important implications for the cosmological evolution of the IGM.

1. Introduction

It has been recognised for many years that powerful extragalactic radio sources of type FR II are ideal tools for probing the universe at early epochs. Because of their enormous luminosity in the radio waveband they can be observed out to very high redshift avoiding the obscuration by dust which complicates observations at other frequencies. The properties and appearance of the large scale structure of FR II sources is influenced by the properties of their environments. An understanding of how powerful radio galaxies and their surroundings interact with each other is therefore crucial for using these objects as local and cosmological probes of the Inter Galactic Matter (IGM).

Plotting the specific radio luminosity of the large scale structure of FR II sources (P) against its linear size (D) one obtains a diagram analogous to the H-R diagram for stars (e.g. Baldwin 1982). However, the presence of Malmquist bias in any flux limited sample (see Figure 1) means that the source distribution in the P-D diagram always reflects the combination of the intrinsic evolution of individual sources and of the cosmological evolution of the FR II source population as a whole. It is therefore necessary to disentangle these two effects in order to determine the cosmological evolution of the radio source environments.

The mechanical energy supplied by an FR II source to its gaseous environment of order 10^{38} W surpasses that of super novae in the host galaxies of these objects. The

¹email: c.kaiser1@physics.oxford.ac.uk

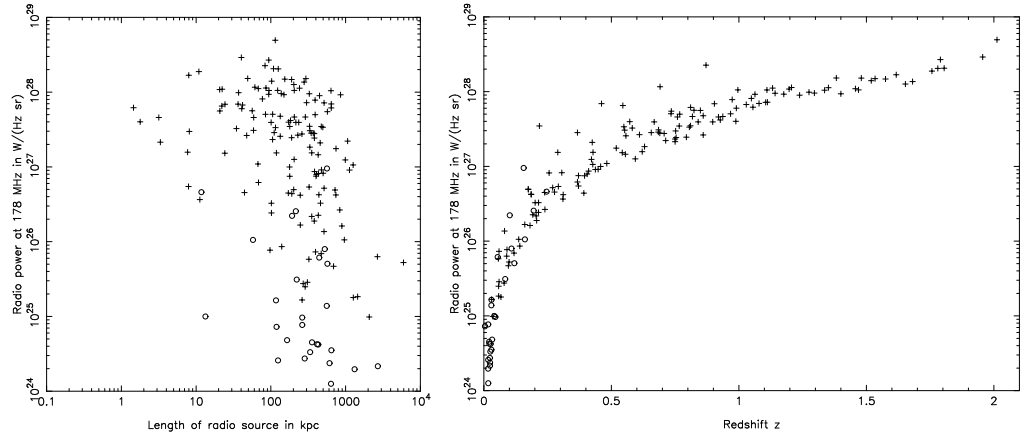


Figure 1. Source distribution in a flux limited sample of radio galaxies (left) and Malmquist bias (right). All sources are taken from the sample defined by Laing, Riley & Longair 1983. Crosses: FRII sources, circles: FRI sources. Note that both diagrams have the same scale in radio luminosity which implies that the more luminous sources are located at higher redshift.

bow shock which is propagating into the IGM in front of the radio cocoon surrounding the jets compresses and heats the IGM (e.g. Scheuer 1974). This compression changes the density profile and also the X-ray emission due to thermal bremsstrahlung of the surrounding gas thereby influencing the subsequent evolution of this material. In the following we will show that the resulting X-ray surface brightness profile reflects the density profile of the unperturbed IGM.

Throughout this paper we will assume $H_o = 50 \text{ km s}^{-1} \text{ Mpc}^{-1}$.

2. Intrinsic source evolution

The basic elements of the large scale structure of an FRII source are sketched in Figure 2. Only one side of a radio source is shown. The jet is assumed to emerge ballistically from the AGN. After passing through the reconfinement shock the jet is in pressure equilibrium with its own cocoon (e.g. Falle 1991, Kaiser & Alexander 1997). The jet ends in a strong jet shock and the jet material subsequently inflates the cocoon. The expansion of the cocoon is supersonic with respect to the IGM and therefore drives a bow shock into this material. Because of the high sound speed within the cocoon the pressure will be uniform in this region except for a small volume surrounding the jet shock, the hot spot region. The material in this region has just been injected by the jet into the cocoon and has therefore had not enough time to ‘communicate’ with the rest of the cocoon. The higher pressure in the hot spot region explains the elongated shape of FRII radio galaxies. The density distribution of the unperturbed IGM is modelled by a simple power law, $\rho_x = \rho_o(r/a_o)^{-\beta}$, where ρ_o is the density at the core radius a_o and r is the distance from the centre of the distribution. Note that this power law is a good approximation to a King (1972) profile of central density ρ_o in the case of distances from the centre greater than a few core radii.

This model predicts self-similar growth of the bow shock and the cocoon. This is supported by observations (e.g. Leahy & Williams 1984, Black 1992). The derived ages for FRII sources agree well with observed spectral ages (Kaiser & Alexander 1997) and the advance speeds of the radio hot spots are within the limits derived by Scheuer (1995) from the asymmetries of observed FRII sources.

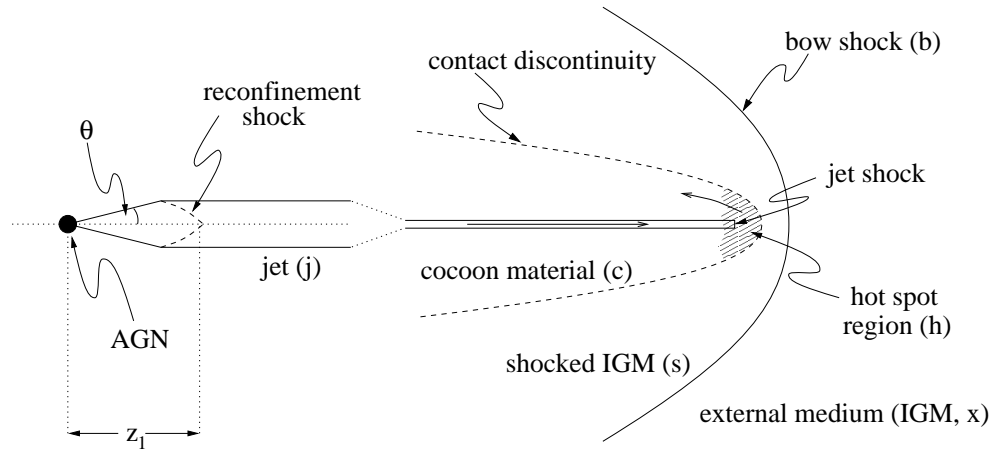


Figure 2. Basic elements of the large scale structure of an FRII source. Reproduced from Kaiser & Alexander 1997.

The radio emission of FRII radio galaxies is created by relativistic electrons within the cocoon radiating via the synchrotron mechanism. These electrons are the subject of energy loss processes which alter the spectrum of the radiation with time. To find the total radio luminosity of the cocoon the time dependent effects of these loss mechanisms have to be taken into account. Kaiser, Dennett-Thorpe & Alexander (1997) present a model in which the cocoon of FRII sources is split up into small volumes characterised by the time of the injection of the relativistic electrons within them into the cocoon. The effects of adiabatic expansion, synchrotron radiation and inverse Compton scattering of the Cosmic Microwave Background Radiation (CMBR) can thereby be traced for these volume elements independently.

With this model it is possible to show that the exact details of the evolution of the magnetic field within the cocoon have no significant effect on the evolutionary tracks of these sources through the P-D diagram. Figure 3 illustrates the influence of redshift and the density of the environment on the shape of the evolutionary tracks. The steepening of the tracks towards larger linear sizes is caused by the increasing importance of inverse Compton scattering. Since the energy density of the CMBR is proportional to $(1+z)^4$, where z is the cosmic redshift, the steepening occurs at smaller linear sizes for sources at higher redshift. This partly explains the observation that the mean linear size of sources at higher redshift is smaller than that of objects at lower redshift (see Figure 1).

The radio luminosity of sources in denser environments is enhanced. The steepening of the tracks occurs at smaller linear sizes for these sources because stronger synchrotron losses have already strongly depleted the number of highly relativistic electrons when inverse Compton scattering becomes important. The assumed shape of the density distribution of the IGM implies that central density, ρ_o , and core radius, a_o , are not independent parameters. The evolutionary tracks only depend on a combination, $\rho_o a_o^\beta$, of the two. This means that the effects of a ‘denser’ environment are indistinguishable from those of a ‘more extended’ environment and Figure 3 may also be interpreted in this way.

3. Cosmological evolution

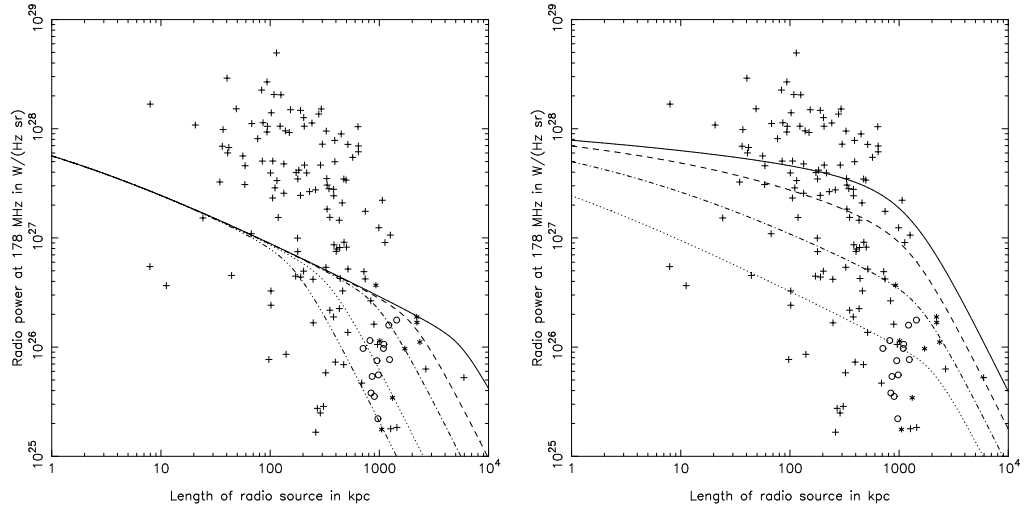


Figure 3. Evolutionary tracks through the P-D diagram as predicted by the model of Kaiser, Dennett-Thorpe & Alexander (1997). Left: Effects of varying the source redshift; solid curve: $z = 0$, dashed: $z = 0.5$, dot-dashed: $z = 1$, dotted: $z = 2$ and dot-dot-dot-dashed: $z = 3$. Right: Varying the external density; the density increases by factors of ten for each curve from bottom to top.

3.1. Modelling the source distribution in the P-D plane

The model for the intrinsic source evolution described in the previous section depends on source parameters (jet power, aspect ratio of the cocoon, distribution of energies of the relativistic electrons at injection, source age, redshift) and parameters describing its environment (external density parameter $\rho_o a_o^\beta$, power law exponent β). All of these parameters are either not directly observable or can only be inferred from observations at comparatively low redshift. The ‘birth function’ of FR II sources, i.e. the comoving number density of progenitors of radio galaxies starting to produce powerful jets as a function of redshift, is of course also unknown. In the following we will assume reasonable distribution functions of these source and environment parameters which initially are assumed to be independent of each other. For the birth function we assume a power law of the form $(1+z)^n$. For a given cosmology it is then possible with the help of the model for the intrinsic radio luminosity-linear size evolution described in the previous section to calculate a continuous distribution function in the P-D plane. This is then compared with the observed, binned source distribution of the complete, flux limited sample of Laing et al. (1983) using a χ^2 -test.

Using this technique we find that the steepening of the evolutionary tracks of FR II sources due to inverse Compton scattering of the CMBR at large linear sizes alone is not sufficient to explain the observed decrease of the median linear size with redshift and/or radio luminosity. More luminous sources at higher redshift tend to host more powerful jets and this also implies higher hot spot advance speeds in these sources. The steepening of their evolutionary tracks therefore occurs only at larger linear sizes; the opposite of what is observed.

Sources in denser environments will not only be more luminous than those in more rarefied surroundings but their expansion speed will be lower as well. The environments of sources at high redshift must have decoupled from the Hubble flow earlier than those of low redshift objects. This very simple picture implies that $\rho_o \propto (1+z)^3$ which leads

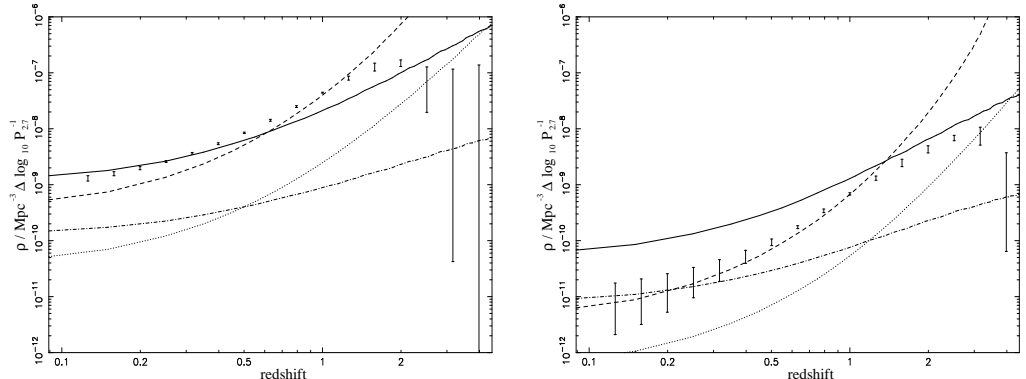


Figure 4. Radio luminosity function as predicted by the two best fitting models for the cosmological evolution of the FRII source population. Left: 10^{26} W Hz $^{-1}$ sr $^{-1}$ at 2.7 GHz, right: 10^{27} W Hz $^{-1}$ sr $^{-1}$ at 2.7 GHz. Solid lines: $\Omega_o = 1$ and model (i) (see text), dashed: $\Omega_o = 1$ and model (ii), dot-dashed: $\Omega_o = 0$ and model (i) and dotted: $\Omega_o = 0$ and model (ii). The error bars show the range of fits to the radio luminosity function using a free modelling approach (Dunlop & Peacock 1990).

to a shortening of the mean size of sources at high redshift. However, we find that this effect is not strong enough.

The single power law assumed for the birth function predicts a monotonously increasing number of sources with increasing redshift. For low radio luminosities the flux limit of the comparison sample means that these sources will not be included in the sample. For high radio luminosities, however, we find that this birth function predicts many more radio luminous sources at high redshift than are observed. This implies at least a flattening, if not a turn over, of the radio luminosity function at redshifts of around 2 which is also indicated by observations (e.g. Dunlop & Peacock 1990).

We find some evidence for a population of giant radio galaxies distinct from the main population by either their exceptionally high age and/or very rarefied environments. There are three, possibly four, sources in the sample of Laing et al. (1983) which have linear sizes close to or above 1.5 Mpc and radio luminosities below 10^{26} W Hz $^{-1}$ sr $^{-1}$ which belong to this class. The probability for finding sources in this region of the P-D diagram is extremely low in any of the models discussed here and their inclusion in the models by allowing for extremely high life times ($> 10^9$ years) leads to an excess of sources with similar sizes but greater radio luminosities which are not observed (see Figure 1).

The disagreement of the model with the observed source distribution suggests that it is necessary to relax the assumption that all source and environment parameters are independent of each other. We find very good agreement between our models and observations for two models: (i) The maximum life time of a source is proportional to $Q_o^{-0.5}$, where Q_o is the jet power, or (ii) the density parameter $\rho_o a_o^\beta$ is proportional to Q_o^2 . Both models predict the correct shortening of the median size with redshift and/or radio luminosity. The radio luminosity function derived from both models is in good agreement with that derived from observations out to about $z = 1.5$ where our simple birth function starts to overpredict the number density of high luminosity sources (Dunlop & Peacock 1990, see Figure 4).

3.2. Interpretation of the cosmological evolution

The sample of Laing et al. (1983) which we used in the previous section to constrain the models of the cosmological evolution of the FRII radio source population includes

only the most luminous objects at any given redshift in the universe. The cosmological evolution of FRII sources and, possibly, their environments we derive from our models therefore only applies to these most luminous objects. This implies that FRII radio galaxies within the model samples defined by the observational flux limit may have widely different intrinsic properties at different redshifts. Indeed we find that the median jet power of sources that should be included in the sample predicted by the models (i) and (ii) increases strongly with redshift; $Q_o \propto (1+z)^5$ for model (i) and $Q_o \propto (1+z)^{5.4}$ for model (ii). Throughout this section it should be borne in mind that we may compare intrinsically different objects at different redshifts with each other in this interpretation.

In model (i) the median environment of sources within the model sample changes only slightly with redshift, $\rho_o a_o^\beta \propto (1+z)^{0.5}$. In model (ii) the environment parameter is proportional to $(1+z)^{10.8}$. If we set the jet power equal to a fraction ϵ of the Eddington luminosity of the black hole in the centre of the AGN producing the jets in a given source, we find that $Q_o \propto \epsilon M_{BH}$, where M_{BH} is the mass of the central black hole. Kormendy & Richstone (1995) find that the mass of the central black hole in quiescent galaxies at low redshift is roughly proportional to the mass of the object it is located in. In the case of spiral galaxies this is the mass of the central bulge while for elliptical galaxies, which are the host galaxies of powerful FRIIs, this is the total mass of the object. The total mass of the progenitor of the radio source is proportional to the density parameter of the environment, $\rho_o a_o^\beta$. Assuming that the relation between total mass and mass of the central black hole extends to higher redshift we find that $\epsilon \propto (1+z)^{4.5}$ in model (i) and $\epsilon \propto (1+z)^{-4.9}$ in model (ii). The jet powers of the most luminous FRII sources at $z = 1$ inferred from radio observations are comparable to the Eddington luminosities of black holes of up to 10^9 solar masses (Rawlings & Saunders 1991). In model (i) this implies an efficiency for the jet production mechanism which is sub-Eddington at low redshift while in model (ii) ϵ is increased at lower redshift. If jets are driven by accretion flows unto black holes, it is unclear how the jet production mechanism can become super-Eddington and this may rule out model (ii). However, if ϵ does not depend on redshift and, say, ρ_o is constant as well we find $a_o \propto (1+z)^{10.8/\beta}$ for model (ii). This means that radio sources should be located in more extended environments at higher redshift. For a decrease in ρ_o with increasing redshift this effect becomes even stronger. There is some observational evidence that the environment of FRII sources may indeed change from poor groups of galaxies at low redshift to richer environments at higher redshift (Hill & Lilly 1991; Best, Longair & Röttgering 1998).

In the scenario of model (ii) the decreasing radio luminosity of the most luminous radio galaxies with decreasing redshift is caused by a decrease in the mass of the central black hole within the jet producing AGN. Since the mass of a super massive black hole will only increase with cosmic time, there should be plenty of objects in the local universe with black holes in their centres which are of comparable or even greater mass than those producing strong radio sources at high redshift. However, at $z \sim 0$ they only give rise to weaker jets creating FRI-type sources or they are quiescent altogether. The most powerful FRII-type objects at low z are always found in poor groups of galaxies. The faster virialisation of the gas in large objects like galaxy clusters as opposed to smaller groups could prevent material from reaching the centre of potential radio source hosts within these rich environments at low redshift and thereby depriving the black holes in these objects of fuel (e.g. Ellingson, Green & Yee 1991). If this scenario is correct, then in any attempt to model the cosmological evolution of the radio galaxy population from hierarchical structure formation it is necessary to take into account not only the presence of a massive black hole but also the availability of fuel for the AGN in potential progenitors of powerful radio galaxies.

To decide which of the two scenarios for the cosmological evolution of the FRII source population is the more appropriate, particularly at lower radio luminosities than those covered by the sample of Laing et al. (1983), it is necessary to use fainter complete samples in the model comparison. These will be available in the near future and should

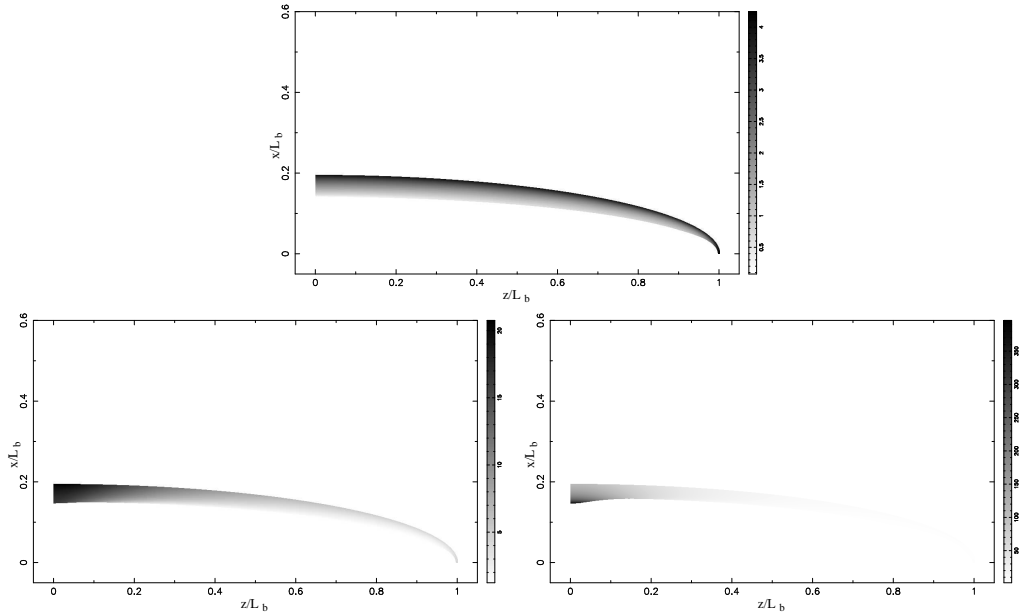


Figure 5. Density distribution of the gas flow between bow shock and cocoon. Only one half of one cocoon is plotted. The core of the AGN where the jets are produced is located in the lower left corner of each panel at $z = 0$ and $x = 0$. The hot spot of the jet is located at $x = 0$ and z just below 1. The bow shock defines the outer edge of the shaded area while the contact discontinuity delineating the cocoon is the inner edge of the same area. Top panel: uniform external density ($\beta = 0$), bottom left: $\beta = 1$ and bottom right: $\beta = 2$.

help to identify the progenitor population of powerful radio galaxies and to constrain the cosmological evolution of their environments.

4. Heating of the IGM

We have pointed out in section 2 that the expansion of the cocoon of FR II sources drives a strong bow shock into the surrounding IGM. The IGM will be compressed and heated by the shock and its properties will change significantly.

The problem of a strong shock expanding into a gaseous atmosphere was first solved for the spherical case in a uniform atmosphere by Sedov (1959). A similar situation but with a constant energy input to a cavity expanding behind the bow shock was investigated by Dyson, Falle & Perry (1980). Both solutions are self-similar and since the expansion of the cocoon and bow shock of FR II radio sources should be self-similar as well (Kaiser & Alexander 1997, Section 2), we expect that these solutions can be extended to this case. The main difference is the elongated shape of the cocoons in FR II sources. By assuming rotational symmetry about the jet axis we can reduce the number of spatial dimension in the problem by one. Transferring the usual equations governing the gas flow between bow shock and cocoon to a self-similarly expanding coordinate system it is possible to transform these equations to a set of partial differential equations in two independent (spatial) coordinates. These can then be solved numerically.

To proceed we have to assume the geometrical shape of the bow shock. The bow shocks in FR II sources can not be observed directly. However, we do not expect the layer of shocked gas between bow shock and cocoon to be very thick and so it seems

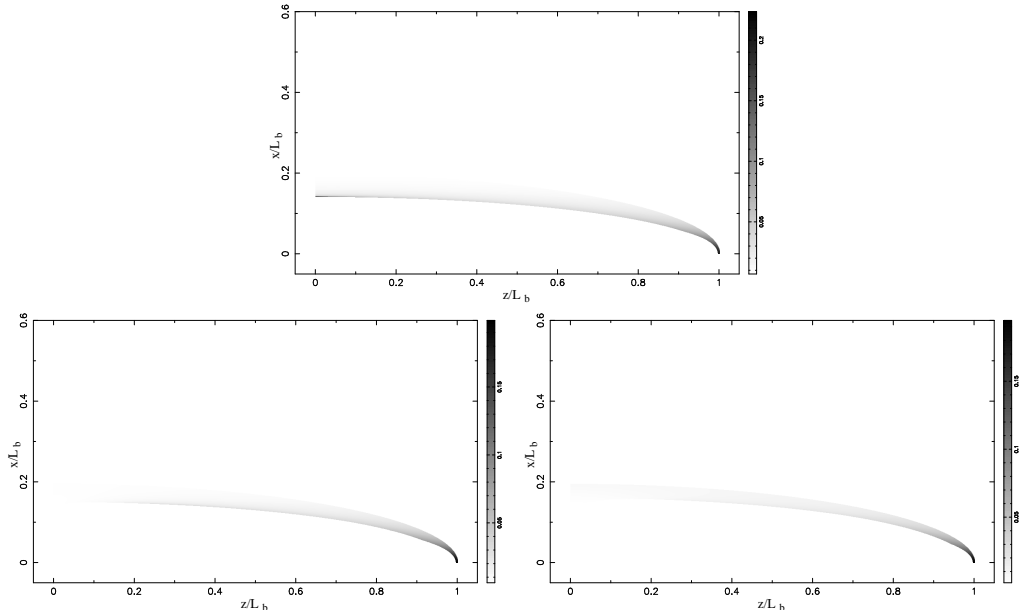


Figure 6. Temperature distribution in the gas between bow shock and cocoon. The orientation of plots is the same as in Figure 5. Top panel: uniform external density ($\beta = 0$), bottom left: $\beta = 1$ and bottom right: $\beta = 2$.

reasonable to assume a prolate ellipsoid shape for the bow shock which resembles the observed shapes of cocoons. At the bow shock surface we assume strong shock conditions which, together with the assumed power law profile for the unperturbed density distribution of the IGM, defines the initial conditions for the integration. The solution is then propagated numerically inwards from the bow shock and stopped at the contact discontinuity. The shape of this surface is not known a priori but can be found using the condition that the gas at the contact discontinuity is not moving in the direction perpendicular to this surface.

Figure 5 shows the result of the integration for various values of the exponent of the external density distribution, β . The shape of the external density distribution is reflected in the flow region. For steep external density gradients, $\beta \sim 2$, the density distribution within the flow region is even steeper than that of the unperturbed gas since in this case the density is rising in the direction from the bow shock toward the cocoon.

We have assumed a power law for the density distribution of the unperturbed IGM. This can be taken as an approximation to an isothermal King (1972) model. The isothermal conditions in the external gas are reflected by the very smooth temperature distribution within the flow region (Figure 6). Only in front of the hot spots we find a somewhat higher temperature.

In section 2 we have shown that the pressure within the cocoon of an FR II source is constant throughout this region except for a small region close to the jet shock where the pressure is higher. The pressure must be matched across the contact discontinuity defining the boundary of the cocoon. From the analysis presented in this section we find that the pressure in the flow between bow shock and cocoon does indeed show a strong decrease in the direction away from the hot spot region. For a uniform external density the pressure along most of the length of the cocoon is almost constant. However, for external density gradients we find the pressure to rise again towards the core of the radio galaxy. For mild gradients, $\beta \sim 1$, this rise is not very strong and would be

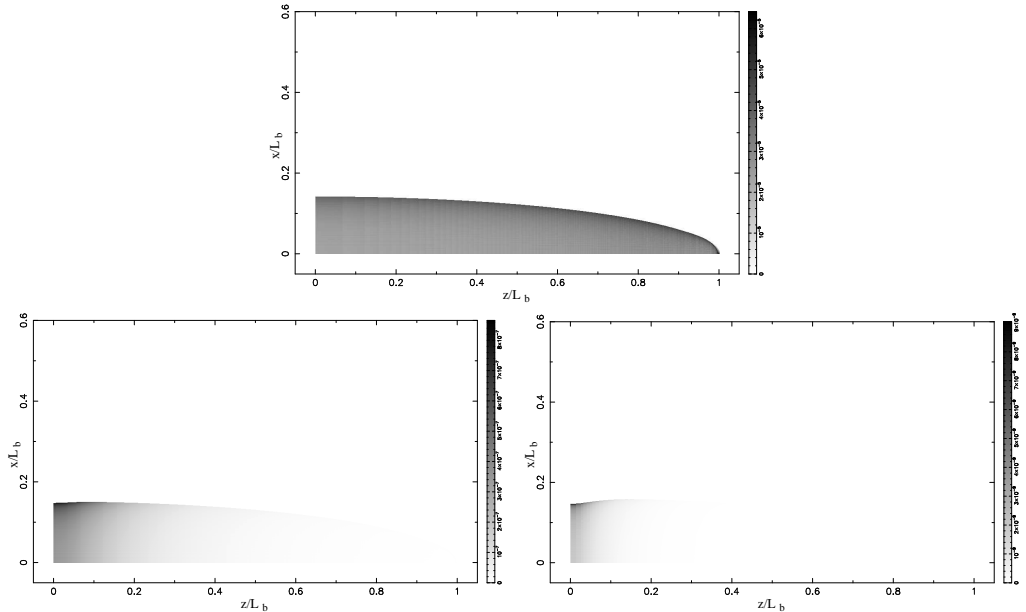


Figure 7. X-ray surface brightness distribution of the gas between bow shock and cocoon. The orientation of plots is the same as in Figure 5. Top panel: uniform external density ($\beta = 0$), bottom left: $\beta = 1$ and bottom right: $\beta = 2$.

expected because of the predictions by numerical simulations of backflow of material within the cocoon (e.g. Norman et al. 1982). In order to avoid gas flow from one side of the radio source to the other there must be a mild, positive pressure gradient towards the core to slow down and stop the backflow within the cocoon. For steeper gradients of the external density this pressure gradient is also steeper which is inconsistent with the high sound speed within the cocoon. The analysis presented here will then apply only as long as the source retains an approximately elliptical shape. However, it is then unlikely that the expansion is self-similar. The further evolution of the source depends on the symmetry of its environment. If the density distribution of the unperturbed IGM is highly symmetric, the shape of the source may still be rotationally symmetric about the jet axis but the pressure equalisation within the cocoon and the region between bow shock and cocoon will lead to a ‘pinching’ of the cocoon towards the core. The shape of the bow shock will then not be elliptical. If the IGM is less symmetrically distributed, significant off axis flow will occur which is commonly observed in FR II sources.

The X-ray emissivity at frequency ν in SI units due to thermal bremsstrahlung of ionised hydrogen is given by (e.g. Shu 1991)

$$\epsilon_\nu = 7 \times 10^{-51} \frac{n_e n_p}{\sqrt{T}} e^{-\frac{h\nu}{kT}} \frac{\text{W}}{\text{m}^3 \text{Hz}}, \quad (1)$$

where n_e and n_p are the electron and proton number density respectively and T is the gas temperature. For observations with a finite bandwidth this is integrated over frequency ν . For Figure 7 we have used the observing band limits of the High Resolution Imager of the ROSAT satellite (0.1 keV \rightarrow 2 keV). To obtain the X-ray surface brightness for a given source from this expression we rotate the source about the jet axis and integrate the emissivity along the line of sight through the source. For simplicity we assume that the source lies exactly in the plane of the sky. Because of the exponential expression in equation (1) the X-ray surface brightness does not scale in a self-similar fashion and we have to choose parameters like the linear size of the source in question. In Figure

7 we show the surface brightness for three sources where we have only changed the exponent of the external density profile between the different panels. Because of the fixed linear size of the sources plotted here the age of the source in the constant density profile (top) is about a factor ten higher than that of the source with $\beta = 2$ (bottom right). A comparison with Figures 5 and 6 shows that the X-ray surface brightness is a good tracer of the gas density within the flow region provided the external gas is isothermal. High resolution, high sensitivity observations of FR II radio galaxies will therefore enable us to constrain the properties of the gaseous environments of these sources at least at low redshift. The cooling times of the shocked IGM between bow shock and cocoon implied by this calculation are comparable or exceed the Hubble time for typical jet and environment parameters. An FR II radio source will therefore influence the evolution of the gas surrounding it far beyond its own limited life time.

It is well known that simulations of the formation of galaxy groups and clusters in the hierarchical structure formation picture predict gas density distributions with cusps at the centre of the distribution (e.g. Navarro, Frenk & White 1995). X-ray observations of the hot gas in clusters reveal flat density profiles at their centres (e.g. Jones & Forman 1984). To reconcile the simulations with the observations additional sources of heat in the cluster centre are invoked such as super nova explosions resulting from early star formation in the cluster progenitors. However, the energy of many super novae is needed to flatten the density profiles in simulations and these super novae would produce high values for the metallicity in the gas of galaxy groups and clusters which is not observed (Ponman in this volume). The enormous amount of mechanical energy transferred by the jets in FR II radio sources to the IGM may explain the observed flattening towards the centre of the density distribution in these objects without producing any additional metallicity.

5. Summary

We have presented models for the intrinsic and cosmological evolution of radio galaxies of type FR II. The observed decrease of the mean linear size of these objects with increasing redshift is explained by two possible scenarios. Either the life time of sources depends on their jet power or the gas in the environments of sources with more powerful jets is denser. The second explanation confirms observational results that FR II radio sources seem to be located in richer environments at higher redshift. This implies that super massive black holes in galaxy clusters in the local universe must be starved of fuel because although they must exist, they do not produce powerful radio sources.

We have also investigated the properties of the flow of shocked gas of the IGM between the bow shock and the cocoon of FR II sources. We have shown that the heating of this material by the bow shock leads to an enhanced emission of X-rays. The resulting distribution of the X-ray surface brightness in the flow reflects the density profile of the material external to the radio source. The expansion of powerful radio galaxies contributes to the energy of the IGM in clusters and groups of galaxies and may constitute the additional source of heat necessary to reconcile numerical simulations of the formation of clusters and groups with the observed properties of the hot gas in these objects.

References

- Baldwin, J. E. 1982, in *Extragalactic radio sources*, D. S. Heeschen, & C. M. Wade, Dordrecht: Reidel, 1982, 21
- Best, P. N., Longair, M. S., & Röttgering, H. J. A. 1998, *MNRAS*, 295, 549
- Black, A. R. S. 1992, Ph.D. thesis, University of Cambridge, 1992
- Dunlop, J. S., & Peacock, J. A. 1990, *MNRAS*, 247, 19

- Dyson, J. E., Falle, S. A. E. G., & Perry, J. J. 1980, MNRAS, 191, 785
Ellingson, E., Green, R. F., & Yee, H. K. C. 1991, ApJ, 378, 476
Falle, S. A. E. G. 1991, MNRAS, 250, 581
Hill, G. J., & Lilly, S. J. 1991, ApJ, 367, 1
Jones, C., & Forman, W. 1984, ApJ, 276, 38
Kaiser, C. R., & Alexander, P. 1997, MNRAS, 286, 215
Kaiser, C. R., Dennett-Thorpe, J., & Alexander, P. 1997, MNRAS, 292, 723
King, I. R. 1972, ApJ, 174, L123
Kormendy, J., & Richstone, D. 1995, ARA&A, 33, 581
Laing, R. A., Riley, J. M., & Longair, M. S. 1983, MNRAS, 204, 151
Leahy, J. P., & Williams, A. G. 1984, MNRAS, 210, 929
Navarro, J. F., Frenk, C. S., & White, S. D. M. 1995, MNRAS, 275, 720
Norman, M. L., Smarr, L., Winkler, K.-H. A., & Smith, M. D. 1982, *Å*, 113, 285
Rawlings, S., & Saunders, R. 1991, Nature, 349, 138
Scheuer, P. A. G. 1974, MNRAS, 166, 513
Scheuer, P. A. G. 1995, MNRAS, 277, 331
Sedov, L.I. 1959, Similarity and dimensional methods in mechanics, Academic Press, 1959
Shu, F. H. 1991, The physics of astrophysics. Vol.1: Radiation, University Science Books, 1991